의학박사 학위논문

# Study on lamina cribrosa parameters - investigation of lamina cribrosa depth and thickness in normal subjects and glaucoma patients

## 사상판 계측에 관한 연구 - 정상안과 녹내장안에서 사상판 깊이와 사상판 두께의 고찰

2016년 2월

서울대학교 대학원

의학과 안과학 전공

서 제 현

**A thesis of the Degree of Doctor of Philosophy in Medical Science (Ophthalmology)**

# 사상판 계측에 관한 연구 - 정상안과 녹내장안에서 사상판 깊이와 사상판 두께의 고찰

# Study on lamina cribrosa parameters - investigation of lamina cribrosa depth and thickness in normal subjects and glaucoma patients

February 2016

The Department of Ophthalmology

Seoul National University

College of Medicine

Je Hyun Seo

# Study on lamina cribrosa parameters - investigation of lamina cribrosa depth and thickness in normal subjects and glaucoma patients

지도교수 김태우

이 논문을 의학박사 학위논문으로 제출함

2015년 10월

서울대학교 대학원

의학과 안과학 전공

서 제 현

서제현의 의학박사 학위논문을 인준함

2016년 1월

| | | |
|---|---|---|
| 위 원 장 | 구 자 원 | (인) |
| 부위원장 | 김 태 우 | (인) |
| 위 원 | 강 성 범 | (인) |
| 위 원 | 박 규 형 | (인) |
| 위 원 | 성 경 림 | (인) |

## Abstract

# Study on lamina cribrosa parameters - investigation of lamina cribrosa depth and thickness in normal subjects and glaucoma patients

Je Hyun Seo
Medicine, Ophthalmology
The Graduate school
Seoul National University

**Purpose**: To investigate the possibility of classifying open angle eyes by lamina cribrosa (LC) depth (LCD) and LC thickness (LCT) using enhanced depth imaging (EDI) spectral domain-optical coherence tomography (SD-OCT).

**Material and Methods:** A total of 335 eyes including 138 open angle eyes from healthy subjects, and 197 patients with open angle glaucoma were enrolled. Serial horizontal B-scans of the optic nerve head were obtained using EDI SD-OCT. LCD (the perpendicular distance from the Bruch's membrane opening plane to the anterior lamina cribrosa surface) and LCT were measured with B-scans from three locations (superior-midperiphery, mid-horizontal, and inferior-midperiphery) in each eye. A hierarchical cluster analysis was performed using the LCD and LCT values. In addition, a logistic regression analysis was performed.

**Results**: The hierarchical cluster analysis yielded three clusters. Cluster 1 was characterized

by a medium LCD (468.06 μm), and medium LCT (166.05 μm). Cluster 2 had the highest LCD (546.40 μm), and the thinnest LCT (146.65 μm). Cluster 3 had the lowest LCD (404.94 μm) and the thickest LCT (201.69 μm). Age, untreated IOP, refractive errors, central corneal thickness, and axial length were different across the clusters.

C**onclusions**: Our hierarchical cluster analysis indicated three clusters in our open angle eye population based on LCD and LCT measurements. These results suggest the possibility of subclassifying open angle eyes, including those with glaucoma, according to LCD and LCT measurements, rather than by IOP results.

**Key words:** Lamina Cribrosa Depth, Lamina Cribrosa Thickness, Hierarchical Cluster Analysis, Spectral Domain Optical Coherence Tomography, Glaucoma

***Student number*: 2012-31123**

# Contents

# List of Tables

# List of Figures

# Introduction

Glaucoma is a progressive optic neuropathy characterized by degeneration of the retinal ganglion cells and their axons. The lamina cribrosa (LC) is considered the putative site of primary axonal injury in glaucoma.[1-4] LC is composed of a delicate net of connective tissue through which the axons of the retinal ganglion cells exit the eye, and provides both structural and functional support.[5] Compression and deformation of the LC are thought to contribute to, or in some instances, initiate, a blockade of axoplasmic flow within the optic nerve fibers, that leads to glaucoma.[1, 6-9] Hence, evaluation of LC structural changes may help improve our understanding of glaucoma pathogenesis.

Numerous experimental studies have shown the posterior displacement of the LC after IOP elevation.[10-13] Several studies have shown that the LC moves anteriorly after lowering the IOP by trabeculectomy[14-16] or deep sclerectomy,[17] and is measured using enhanced depth imaging (EDI) spectral domain-optical coherence tomography (SD-OCT). These findings suggest that displacement and/or thinning of the LC is a principal component of glaucomatous optic neuropathy in the human eye. Hence, it is essential to investigate the architecture of the LC in glaucoma to understand the pathogenesis of the disease. Several investigators have shown that LC depth (LCD, as a parameter reflecting backward bowing) to be a new LC parameter for LC study, and a useful parameter for studying primary open angle glaucoma (POAG).[18-24]In addition, several studies on LC thickness (LCT, as a parameter reflecting compression) in eyes with glaucoma and normal eyes found that the LCT in eyes with glaucoma was thinner than that of normal eyes.[16, 25-29]

POAG is the most commonly studied type of glaucoma, however, its pathogenesis remains unclear.[30] Several mechanisms have been suggested and remain the subject of debate.[31-36] Recently, our previous study demonstrated that a thinner LCT and a larger LCD

had a significant influence on the rate of progressive retinal nerve fiber layer thinning in POAG.[37] Thus, we hypothesized that open angle eyes with glaucoma and healthy controls can be subclassified by LCD and LCT measurements. The purpose of this study was to investigate the possibility of classifying open angle eyes by LCD and LCT using EDI SD-OCT.

# Materials and Methods

This study was conducted on healthy subjects and patients with glaucoma attending the Seoul National University Bundang Hospital Glaucoma Clinic from June 2010 to March 2014. The study was approved by the Seoul National University Bundang Hospital Institutional Review Board and conformed to the Declaration of Helsinki. Informed consent was obtained from all subjects.

**Study Subjects**

The normal subjects were enrolled by advertisement, and patients with consecutive open angle glaucoma, as confirmed by the presence of glaucomatous visual field defects, were recruited to the study. All participants underwent complete ophthalmic examinations including visual acuity measurements, Goldmann applanation tonometry, refraction, slit-lamp biomicroscopy, gonioscopy, stereoscopic disc photography (EOS D60 digital camera;Canon, Utsunomiyashi, Tochigiken, Japan), SD-OCT (Spectralis; Heidelberg Engineering, Heidelberg, Germany), central corneal thickness measurements (Orbscan II, Bausch & Lomb Surgical, Rochester, NY), axial length measurements (IOL Master ver.5, Carl Zeiss Meditec, Dublin, CA) and standard automated perimetry (Humphrey Field Analyzer II 750; 24-2 Swedish interactive threshold algorithm; Carl-Zeiss Meditec).

Subjects were required to meet the following criteria to be included in the study: at least two IOP measurements before their anti-glaucoma treatment, a best-corrected visual acuity of 20/40 or better, a spherical equivalent refractive error range from -7.0D to +3.0D, a cylinder correction lesser than ± 3.0D, open anterior chamber angle, and reliable visual fields (fixation loss rate ≤ 20%, false-positive and false-negative error rates ≤ 25%).

The normal eyes were defined as having an IOP level below 21 mmHg without anti-glaucoma medication, an open iridocorneal angle, normal appearing optic discs, and normal

visual fields. Normal appearing optic discs were defined as the absence of glaucomatous optic neuropathy (i.e., focal thinning, notching, and disc hemorrhage), and the absence of pallor or swelling of the optic disc. Normal visual fields were defined as the absence of glaucomatous or neurologic visual field defects. A POAG eye was defined as having glaucomatous optic neuropathy, such as rim thinning, notching and retinal nerve fiber layer (RNFL) defect, glaucomatous visual field defects, and an open iridocorneal angle. Glaucomatous visual field defects were defined as follows: an outside the normal limit on glaucoma hemifield test; or, three abnormal points with P < 5 % probability of being normal, one with P < 1 % by pattern deviation; or, a pattern standard deviation < 5 %, confirmed by two consecutive tests. A visual field measurement was considered reliable when the false-positive/negative results were < 25%, and fixation losses were < 20%.

Subjects with a history of ocular surgery other than uncomplicated cataract surgery, history of ocular trauma and uveitis, or other diseases affecting the visual field (e.g. diabetic retinopathy, retinal vein occlusion, ischemic optic neuropathy), were excluded. Eyes with optic disc torsion of more than 15°,[38] or a tilt ratio (minimum-to-maximal optic disc diameter) less than 0.75,[39] were excluded from this study. Subjects yielding poor OCT quality images, as described below (see enhanced depth imaging OCT section), were also excluded.

**Enhanced Depth Imaging (EDI) OCT**

The optic nerve images were acquired by a Spectralis OCT, using the EDI technique. The details and advantages of this technology in evaluating the LC have been described previously.[40-42] In brief, the imaging was performed using a 10° x 15°rectangle covering the optic disc. This rectangle was scanned with approximately 65 sections, which were 30 to 34 μm apart (the slicing distance is determined automatically by the machine). Each section had 42 OCT frames averaged, which optimized the balance between image quality and

patient cooperation. When using the Spectralis OCT, the images are obtainable only when the quality score is greater than 15. When the quality score does not reach 15, the image acquisition process automatically stops and image of the respective section remains blank. Eyes were excluded when a good quality image (i.e. quality score > 15) could not be obtained for more than five sections. Moreover, subjects were excluded when the image did not allow clear delineation of the anterior border of the central LC. Three-dimensional (3D) volumetric images were reconstructed from the B-scan images;en face images were constructed from the 3D images using image-processing software (Amira 5.2.2, Visage Imaging, Berlin, Germany).

## Measurement of Lamina Cribrosa Depth and Lamina Cribrosa Thickness

After the 3D image was reconstructed, LCD and LCT were measured with B-scans from three locations (superior-midperiphery, mid-horizontal, and inferior-midperiphery) in each eye. Lamina cribrosa depth was defined as the perpendicular distance from the Bruch's membrane opening plane to the anterior lamina cribrosa surface (ALCS). To do this, a line connecting the Bruch's membrane edges was set as a reference plane, then, the LCD was measured in the direction perpendicular to that reference plane. A smooth contour line was drawn following the ALCS; the maximum depth was measured as the LCD in each B-scan (**Figure 1-A**). The mean LCD of the eye was defined as the average of the LCDs from the three locations.

The lamina cribrosa thickness was measured at three locations in each eye, using thin-slab maximum intensity projection (MIP) images. The thin-slab MIP images were used because they allow for detection of a straighter posterior LC border.[43] The LCT (**Figure 1-B**) was determined as the distance between the anterior and the posterior borders of the highly reflective region. When the anterior or posterior border of the lamina cribrosa was not

clearly defined on the B-scan image, the borders were determined by examining the en face images. The average of the LCT from the three locations was defined as the mean LCT of the eye.

Each B-scan image was enlarged on a computer screen so that each pixel was clearly visible when the caliper tool was used. The LCD and LCT were measured using Amira 5.2.2 software by a single experienced observer (JHS) who was blind to the clinical information. Our previous study showed that the inter-observer intra-class correlation coefficient (ICC) of this method was more than 0.998.[16]

**Data Analysis**

A hierarchical cluster analysis was used to classify the open angle eyes using the lamina parameters LCD and LCT. Among the several options in determining a strategy for merging clusters, Ward's minimum variance method was used as the clustering criterion. All variables were standardized before clustering, particularly the LCD and LCT. In addition, other variables, such as age, sex, IOP, RNFL thickness, spherical equivalents, CCT, and AXL, were included in the hierarchical clustering analysis. To determine k as the optimal number of clusters, two statistical values were examined: first, the biggest drop of semi-partial $R^2$ at k clusters compared with k-1 clusters, and second, the maximum pseudo F statistic at k clusters.

Each cluster was characterized by the differences in variables among the clusters; additional parameters were also compared among clusters. One-way analysis of variance was used to analyze the differences among clusters, and Turkey's post hoc test was performed to establish statistical significance between groups. In addition, we calculated a classification tree and its accuracy. A logistic regression analysis was performed to assess the glaucoma association ability for LCD and LCT. Statistical analysis was performed using

the R Statistical Package, Version 3.03 (R Foundation for Statistical Computing, Vienna, Austria).

# Results

The study initially involved 140 eyes from normal subjects and 200 eyes from patients with glaucoma who were willing to participate in the study. Of these, five subjects (two normal subjects and three patients with glaucoma) were excluded, due to low image quality that disabled a clear delineation of the anterior border of the LC. Finally, 335 eyes from 138 normal subjects and 197 POAG patients were enrolled (**Table 1**). The age of the glaucoma group was older than the normal subjects group (60.04 ± 14.28 versus 48.56 ± 14.11, $P <$ 0.0001).The untreated IOP levels and IOP levels at scan day from patients with glaucoma were higher than those from the normal subject ($Ps < 0.0001$).The glaucoma group showed more myopic refractive errors and higher axial lengths than the normal subjects ($P = 0.003$, $P = 0.004$, respectively). Comparisons of sex and CCT did not reveal statistical differences between glaucoma group and normal subjects ($P = 0.374$, $P = 0.774$, respectively).

## Hierarchical Cluster Analysis

When the optimal cluster number (k) was three, the drop of semi-partial $R^2$ was greatest at k clusters (0.062) compared with k-1 clusters (0.124), and the pseudo F statistic peaked at k clusters (**Table 2**). Hierarchical cluster analysis identified three as the best number of clusters, with 0.290 $R^2$ values in the dendrogram (**Figure 2**). Cluster 1 contained 89 eyes and showed medium range LCDs (468.06 ± 109.84μm) and LCTs (166.05 ± 30.49μm), among all clusters (**Table 3**). Cluster 2 (130 eyes) showed the deepest LCD (546.40 ± 135.99 μm) and the thinnest LCT (146.65 ± 30.34 μm). Cluster 3 (116 eyes) showed the shallowest LCD (404.94 ± 95.45 μm) and the thickest LCT (201.69 ± 14.18 μm) among all the clusters.

The mean age in cluster 2 was 65.07 ±13.44 years old, which was significantly older than that of clusters 1 and 3 ($P < 0.0001$, **Table 4**). The three clusters did not show statistical

differences across sex (*Ps* > 0.999). The untreated IOP in cluster 2 was significantly higher than that of cluster 1 (21.03 ± 9.50 versus 16.68 ± 4.75 mmHg, *P* < 0.0001, respectively). In addition, the untreated IOPs in cluster 1 were higher than those of cluster 3 (12.53 ± 2.37 mmHg, *P* < 0.0001). The IOP at scan day in cluster 2 (16.00 ± 7.65 mmHg) was higher than that of clusters 1 (13.84 ± 4.53 mmHg, *P* = 0.121) and 3 (12.51 ± 2.35 mmHg, *P* < 0.0001). Refractive errors showed more myopic eyes in clusters1 (-4.29 ± 2.52 D) than that in clusters 2 (-0.19 ± 1.72 D, *P* < 0.0001) and 3 (0.52 ± 1.40 D, *P* < 0.0001). CCT levels in cluster 1 were thinner than those in clusters 2 and 3 (*P* = 0.0025, 0.0414, respectively). The AXL in cluster 1 were longer than those in clusters 2 and 3 (*Ps* < 0.0001). The average RNFL thickness from the OCT and the mean deviation (MD) values from visual field examination were significantly different across all clusters (*Ps* < 0.0001).

## Classification Tree & Cluster Plot

A classification tree was drawn for **Figure 3**. In brief, persons with LCT values greater than 183.9 μm were categorized as cluster 3. Persons with LCTs equal to or less than 183.9 μm were divided by LCDs value (562.5 μm); Persons with LCDs greater than 562.5 μm were classified as cluster 2. Of the remaining persons, those with LCTs greater than 146.8 μm were classified as cluster 1, and those with LCTs equal or less than 146.8 μm were classified as cluster 2. The classification tree accuracy was 0.704 (**Table 5**).

## Logistic Regression Analysis

Logistic regression analysis showed that both LCD and LCT were significantly related to glaucoma (*P* = 0.0004, *P* <0.0001, **Table 6**). When LCD increased one μm, the odds-ratio of glaucoma increased to 1.0067. When LCT increased one μm, the odds-ratio of glaucoma decreased to 0.9038. The accuracy of the logistic regression analysis was 89.0 %.

# Discussion

The optic nerve head (ONH) consists of neural, vascular, and connective tissue. The connective tissues of the ONH are load-bearing tissues of the peripapillary sclera, sclera canal wall, and LC. The displacement of the anterior LC surface has been reported in animal experiments and clinical studies with IOP changes.[6, 31, 44-46] In addition, the backward bowing, as well as compression of LC sheets, are principal features of glaucoma.[3] Given that the posterior displacement of the LC is major component of LC deformation in glaucoma, it is essential to understand LCD in glaucoma. Several researchers have reported that the LCT is different between POAG with normal pressure and POAG with high pressure.[25, 28] In their study, the diagnostic capability of LCT for glaucoma was comparable to that of peripapillary RNFL thickness for glaucoma.[25] Thus, measurements of the LCD and LCT are potentially useful indices for investigating glaucoma pathogenesis.

We evaluated the LC features *in vivo* (LC depth and LC thickness) of open angle eyes in POAG subjects and healthy subjects using a hierarchical cluster analysis. Our analysis indicated three clusters with different characteristics of LCD and LCT. To our knowledge, this study is the first study regarding the use of LC parameters for glaucoma classification using a hierarchical cluster analysis. Some researchers may consider POAG classification according to IOP level arbitrary; however, we believe it is necessary and worthwhile to examine IOP levels when investigating glaucoma. Of the POAG cases with normal pressure, 42.4 % were located in cluster 1, 56.1 % in cluster 2, and 1.5% in cluster 3. Of the POAG cases with high pressure, 20 % were located in cluster 1, 80 % located in cluster 2, and 0% in cluster 3. Within the normal subject group, 14.5% were located in cluster 1, 2.9 % in cluster 2, and 82.6% in cluster 3. These results support that the classification of POAG according to baseline IOP levels would be arbitrary work.

Cluster 1 (89 eyes) showed a medium range of LCD and LCT among the clusters. Cluster 1 consisted of 56 POAG with normal pressure (62.9 %), 13 POAG with high pressure (14.6 %), and 20 normal subjects (22.5%). This cluster is a relatively heterogeneous group dominantly composed of POAG with normal pressure. This may be due to the overlap in LCD and LCT between POAG in its early glaucoma stage and normal subjects. The untreated IOP and IOP at scan day in cluster 1 were lower than those of cluster 2. And, CCT was thinnest in cluster 1. This thin CCT may be related to the lower baseline IOP. Interestingly, this cluster contained the younger age group and myopic eyes. This point is consistent with the results of a previous study, that myopia is a risk factor for glaucoma development.[47-49] In this study, cluster 1 looked as heterogeneous group. This finding suggests that additional parameter may be helpful for more detailed clustering. Recently, some studies suggested other LC-related parameters, including peripheral lamina cribrosa depth, LC curvature, BMO-minimum rim width as potential factors relevant with ONH biomechanics.[50, 51] We consider that these parameters combined with LCT and LCD may enable further categorization of POAG patients.

Cluster 2 (130 eyes) showed the largest LCD and the thinnest LCT. It consisted of 74 POAG cases with normal pressure (56.9 %), 52 POAG cases with high pressure (40.0 %), and 4 normal subjects (3.0 %). This cluster is predominantly composed of higher baseline IOPs than in clusters 1 or 3. Cluster 2 was composed of the older age group, and consisted of advanced glaucoma cases with lower ranges of RNFL thickness and MD values of the visual field, as compared to cluster 1. This cluster showed characteristics of an advanced glaucoma group. These results demonstrate that LCD and LCT changes are related to glaucoma progression, which is consistent with results from a previous study.[37] Elevated IOP in POAG was still an important factor in the disease progression. Cluster 3 (116 eyes)

showed the shallowest LCD and the thickest LCT among the clusters. This group consisted of two POAG cases with normal pressure (1.7 %) and 114 normal subjects (98.3 %). Cluster 3 consisted predominantly of normal subjects.

Recently, Lee *et al.* indicated that thinner LCT and larger LC displacement had significant influence on the rate of progressive RNFL thinning.[37] In their results, the breakpoint for LCD was 489.7 μm, above which a faster rate of global RNFL thinning was associated with a larger LCD. These findings concur that our result, that a LCD cut-off value of 562.5 μm between clusters 1 and 2 delineates cluster 2 as being the faster progression group.

In our study, cluster 2 contained more advanced stage glaucoma cases and showed deeper LCD and thinner LCT than cluster 1. This report demonstrates that both LCD and LCT are related to the stage of glaucoma. These results are consistent with reports of Park *et al*., that LC deepening developed in preperimetric glaucoma and early stage glaucoma.[51] They suggested that LCD had limited value in comparison between moderate stage and advanced stages of glaucoma. Other study evaluated the diagnostic ability of LCT for NTG and POAG, and showed that LCT is correlated with glaucoma stages, even at advanced stages.[25, 28] Although LCT was significantly different between the NTG and POAG cases in their study,[25] our cluster analysis showed that it was difficult to clearly divide POAG with high pressure and NTG with LCD and LCT measurements.

Our study has several limitations. First, all included subjects were Korean. Given the ethnic difference in the optic disc topography,[52] it is likely that there is an ethnic variation in the LCD, and LCT. Further study is needed in other ethnic groups. Second, our study population did not include patients with ocular hypertension. This group would have different LCD and LCT measurements than the patients with glaucoma or healthy subject. Therefore, further studies with patients with ocular hypertension, or acute angle closure are

needed. Third, LCD was measured by EDI OCT with a reference line connecting the Bruch's membrane edges. Recently, improvements in EDI OCT imaging techniques have allowed for better images of deeper eye structures, including the LC configuration and structure in normal eyes and glaucoma. Swept-source OCT has a longer central wavelength, improving its tissue penetration over conventional OCT. The detection rate of the posterior border of the sclera was higher in swept-source OCT than in EDI OCT. Hence, it would be better to measure LCD using swept-source OCT. Forth, focal LC changes were not considered for this study, as defects of the LC were related to localized RNFL defects.[53] Although, this study was intended for whether LCD and LCT can categorize glaucoma, focal LC changes potentially can be a parameter of LC evaluation. In addition, inclusion of other risk factors – disc hemorrhage, peripapillary atrophy, and ocular torsion would enrich our study. To resolve this problem, further study is needed.

In conclusion, we demonstrated the hierarchical cluster analysis of open angle eyes yielded three groups based on LC parameters, LCD and LCT, as assessed by SD-OCT. This study attempted to build a new classification of POAG according to LCD and LCT, which may be related to the pathological classification.

# References


1. Jonas JB, Berenshtein E, Holbach L. Lamina cribrosa thickness and spatial relationships between intraocular space and cerebrospinal fluid space in highly myopic eyes. *Invest Ophthalmol Vis Sci* 2004;45:2660-2665.

2. Jonas JB, Berenshtein E, Holbach L. Anatomic relationship between lamina cribrosa, intraocular space, and cerebrospinal fluid space. *Invest Ophthalmol Vis Sci* 2003;44:5189-5195.

3. Quigley HA, Hohman RM, Addicks EM, Massof RW, Green WR. Morphologic changes in the lamina cribrosa correlated with neural loss in open-angle glaucoma. *Am J Ophthalmol* 1983;95:673-691.

4. Quigley HA, Addicks EM, Green WR, Maumenee AE. Optic nerve damage in human glaucoma. II. The site of injury and susceptibility to damage. *Arch Ophthalmol* 1981;99:635-649.

5. Morgan WH, Yu DY, Cooper RL, Alder VA, Cringle SJ, Constable IJ. The influence of cerebrospinal fluid pressure on the lamina cribrosa tissue pressure gradient. *Invest Ophthalmol Vis Sci* 1995;36:1163-1172.

6. Bellezza AJ, Rintalan CJ, Thompson HW, Downs JC, Hart RT, Burgoyne CF. Deformation of the lamina cribrosa and anterior scleral canal wall in early experimental glaucoma. *Invest Ophthalmol Vis Sci* 2003;44:623-637.

7. Jonas JB, Mardin CY, Schlotzer-Schrehardt U, Naumann GO. Morphometry of the human lamina cribrosa surface. *Invest Ophthalmol Vis Sci* 1991;32:401-405.

8. Dandona L, Quigley HA, Brown AE, Enger C. Quantitative regional structure of the normal human lamina cribrosa. A racial comparison. *Arch Ophthalmol* 1990;108:393-398.

9. Radius RL, Gonzales M. Anatomy of the lamina cribrosa in human eyes. *Arch Ophthalmol* 1981;99:2159-2162.

10. Strouthidis NG, Fortune B, Yang H, Sigal IA, Burgoyne CF. Effect of acute intraocular pressure elevation on the monkey optic nerve head as detected by spectral domain optical coherence tomography. *Invest Ophthalmol Vis Sci* 2011;52:9431-9437.

11. Fortune B, Choe TE, Reynaud J, et al. Deformation of the rodent optic nerve head and peripapillary structures during acute intraocular pressure elevation. *Invest Ophthalmol Vis Sci* 2011;52:6651-6661.

12. Fatehee N, Yu PK, Morgan WH, Cringle SJ, Yu DY. The impact of acutely elevated intraocular pressure on the porcine optic nerve head. *Invest Ophthalmol Vis Sci* 2011;52:6192-6198.

13. Girard MJ, Downs JC, Burgoyne CF, Suh JK. Experimental surface strain mapping of porcine peripapillary sclera due to elevations of intraocular pressure. *J Biomech Eng* 2008;130:041017.

14. Lee EJ, Kim TW, Weinreb RN, Kim H. Reversal of lamina cribrosa displacement after intraocular pressure reduction in open-angle glaucoma. *Ophthalmology* 2013;120:553-559.

15. Lee EJ, Kim TW, Weinreb RN. Variation of lamina cribrosa depth following trabeculectomy. *Invest Ophthalmol Vis Sci* 2013;54:5392-5399.

16. Lee EJ, Kim TW, Weinreb RN. Reversal of lamina cribrosa displacement and thickness after trabeculectomy in glaucoma. *Ophthalmology* 2012;119:1359-1366.

17. Barrancos C, Rebolleda G, Oblanca N, Cabarga C, Munoz-Negrete FJ. Changes in lamina cribrosa and prelaminar tissue after deep sclerectomy. *Eye (Lond)* 2014;28:58-65.

18. Sigal IA, Grimm JL, Jan NJ, Reid K, Minckler DS, Brown DJ. Eye-specific IOP-

induced displacements and deformations of human lamina cribrosa. *Invest Ophthalmol Vis Sci* 2014;55:1-15.

19. Seo JH, Kim TW, Weinreb RN. Lamina cribrosa depth in healthy eyes. *Invest Ophthalmol Vis Sci* 2014;55:1241-1251.

20. Ren R, Yang H, Gardiner SK, et al. Anterior lamina cribrosa surface depth, age, and visual field sensitivity in the portland progression project. *Invest Ophthalmol Vis Sci* 2014;55:1531-1539.

21. Jung KI, Jung Y, Park KT, Park CK. Factors affecting plastic lamina cribrosa displacement in glaucoma patients. *Invest Ophthalmol Vis Sci* 2014.

22. Park SC, Hsu AT, Su D, et al. Factors associated with focal lamina cribrosa defects in glaucoma. *Invest Ophthalmol Vis Sci* 2013;54:8401-8407.

23. Park SC. In vivo evaluation of lamina cribrosa deformation in glaucoma. *J Glaucoma* 2013;22 Suppl 5:S29-31.

24. Park SC, Kiumehr S, Teng CC, Tello C, Liebmann JM, Ritch R. Horizontal central ridge of the lamina cribrosa and regional differences in laminar insertion in healthy subjects. *Invest Ophthalmol Vis Sci* 2012;53:1610-1616.

25. Park HY, Park CK. Diagnostic capability of lamina cribrosa thickness by enhanced depth imaging and factors affecting thickness in patients with glaucoma. *Ophthalmology* 2013;120:745-752.

26. Lee EJ, Kim TW, Weinreb RN, Suh MH, Kim H. Lamina cribrosa thickness is not correlated with central corneal thickness or axial length in healthy eyes: central corneal thickness, axial length, and lamina cribrosa thickness. *Graefes Arch Clin Exp Ophthalmol* 2013;251:847-854.

27. Park SC, De Moraes CG, Teng CC, Tello C, Liebmann JM, Ritch R. Enhanced

depth imaging optical coherence tomography of deep optic nerve complex structures in glaucoma. *Ophthalmology* 2012;119:3-9.

28. Park HY, Jeon SH, Park CK. Enhanced depth imaging detects lamina cribrosa thickness differences in normal tension glaucoma and primary open-angle glaucoma. *Ophthalmology* 2012;119:10-20.

29. Lee EJ, Kim TW, Weinreb RN, et al. Three-dimensional evaluation of the lamina cribrosa using spectral-domain optical coherence tomography in glaucoma. *Invest Ophthalmol Vis Sci* 2012;53:198-204.

30. Kwon YH, Fingert JH, Kuehn MH, Alward WL. Primary open-angle glaucoma. *N Engl J Med* 2009;360:1113-1124.

31. Burgoyne CF, Downs JC, Bellezza AJ, Suh JK, Hart RT. The optic nerve head as a biomechanical structure: a new paradigm for understanding the role of IOP-related stress and strain in the pathophysiology of glaucomatous optic nerve head damage. *Prog Retin Eye Res* 2005;24:39-73.

32. Soares AS, Artes PH, Andreou P, Leblanc RP, Chauhan BC, Nicolela MT. Factors associated with optic disc hemorrhages in glaucoma. *Ophthalmology* 2004;111:1653-1657.

33. Sigal IA, Flanagan JG, Tertinegg I, Ethier CR. Finite element modeling of optic nerve head biomechanics. *Invest Ophthalmol Vis Sci* 2004;45:4378-4387.

34. Galloway PH, Warner SJ, Morshed MG, Mikelberg FS. Helicobacter pylori infection and the risk for open-angle glaucoma. *Ophthalmology* 2003;110:922-925.

35. Yamamoto T, Kitazawa Y. Vascular pathogenesis of normal-tension glaucoma: a possible pathogenetic factor, other than intraocular pressure, of glaucomatous optic neuropathy. *Prog Retin Eye Res* 1998;17:127-143.

36. Jonas JB, Grundler AE, Gonzales-Cortes J. Pressure-dependent neuroretinal rim

loss in normal-pressure glaucoma. *Am J Ophthalmol* 1998;125:137-144.

37. Lee EJ, Kim TW, Kim M, Kim H. Influence of lamina cribrosa thickness and depth on the rate of progressive retinal nerve fiber layer thinning. *Ophthalmology* 2015;122:721-729.

38. Vongphanit J, Mitchell P, Wang JJ. Population prevalence of tilted optic disks and the relationship of this sign to refractive error. *Am J Ophthalmol* 2002;133:679-685.

39. Jonas JB, Kling F, Grundler AE. Optic disc shape, corneal astigmatism, and amblyopia. *Ophthalmology* 1997;104:1934-1937.

40. Lee EJ, Kim TW, Weinreb RN, Park KH, Kim SH, Kim DM. Visualization of the lamina cribrosa using enhanced depth imaging spectral-domain optical coherence tomography. *Am J Ophthalmol* 2011;152:87-95 e81.

41. Inoue R, Hangai M, Kotera Y, et al. Three-dimensional high-speed optical coherence tomography imaging of lamina cribrosa in glaucoma. *Ophthalmology* 2009;116:214-222.

42. Spaide RF, Koizumi H, Pozzoni MC. Enhanced depth imaging spectral-domain optical coherence tomography. *Am J Ophthalmol* 2008;146:496-500.

43. Lee EJ, Kim TW, Weinreb RN. Improved reproducibility in measuring the laminar thickness on enhanced depth imaging SD-OCT images using maximum intensity projection. *Invest Ophthalmol Vis Sci* 2012;53:7576-7582.

44. Strouthidis NG, Fortune B, Yang H, Sigal IA, Burgoyne CF. Longitudinal change detected by spectral domain optical coherence tomography in the optic nerve head and peripapillary retina in experimental glaucoma. *Invest Ophthalmol Vis Sci* 2011;52:1206-1219.

45. Yang H, Downs JC, Girkin C, et al. 3-D histomorphometry of the normal and early

glaucomatous monkey optic nerve head: lamina cribrosa and peripapillary scleral position and thickness. *Invest Ophthalmol Vis Sci* 2007;48:4597-4607.

46. Burgoyne CF, Downs JC, Bellezza AJ, Hart RT. Three-dimensional reconstruction of normal and early glaucoma monkey optic nerve head connective tissues. *Invest Ophthalmol Vis Sci* 2004;45:4388-4399.

47. Kim MJ, Kim MJ, Kim HS, Jeoung JW, Park KH. Risk factors for open-angle glaucoma with normal baseline intraocular pressure in a young population: the Korea National Health and Nutrition Examination Survey. *Clin Experiment Ophthalmol* 2014.

48. Qiu M, Wang SY, Singh K, Lin SC. Association between myopia and glaucoma in the United States population. *Invest Ophthalmol Vis Sci* 2013;54:830-835.

49. Mitchell P, Hourihan F, Sandbach J, Wang JJ. The relationship between glaucoma and myopia: the Blue Mountains Eye Study. *Ophthalmology* 1999;106:2010-2015.

50. Thakku SG, Tham YC, Baskaran M, et al. A Global Shape Index to Characterize Anterior Lamina Cribrosa Morphology and Its Determinants in Healthy Indian Eyes. *Invest Ophthalmol Vis Sci* 2015;56:3604-3614.

51. Park SC, Brumm J, Furlanetto RL, et al. Lamina cribrosa depth in different stages of glaucoma. *Invest Ophthalmol Vis Sci* 2015;56:2059-2064.

52. Tsai CS, Zangwill L, Gonzalez C, et al. Ethnic differences in optic nerve head topography. *J Glaucoma* 1995;4:248-257.

53. Tatham AJ, Miki A, Weinreb RN, Zangwill LM, Medeiros FA. Defects of the lamina cribrosa in eyes with localized retinal nerve fiber layer loss. *Ophthalmology* 2014;121:110-118.

**Table 1. Demographic Data of Enrolled Subjects**

| | Normal subject N=138 | Glaucoma patients N=197 | *P*-value* |
|---|---|---|---|
| Age, y | 48.56 ± 14.11 | 60.04 ± 14.28 | <0.0001 |
| Sex, male/female | 61 / 77 | 98 / 99 | 0.374 |
| Untreated IOP, mmHg | 12.66 ± 2.52 | 19.93 ± 8.32 | <0.0001 |
| IOP at scan day, mmHg | 12.66 ± 2.52 | 15.32 ± 6.89 | <0.0001 |
| Refractive errors, D | -0.90 ± 1.91 | -1.74 ± 2.88 | 0.003 |
| CCT, μm | 554.97 ± 37.11 | 553.76 ± 38.88 | 0.774 |
| AXL, mm | 23.86 ± 1.09 | 24.29 ± 1.49 | 0.004 |
| Average RNFL thickness, μm | 101.51 ± 9.32 | 66.47 ± 16.08 | <0.0001 |
| MD, dB | -0.44 ± 1.15 | -10.29 ± 8.43 | <0.0001 |

IOP=Intraocular pressure, D=Diopter, CCT=Central corneal thickness, AXL=Axial length, RNFL=Retinal nerve fiber layer, MD=Mean deviation.

* *P*-value by analysis of independent T test for variables, in case of numeric, Chi-square test was applied.

**Table 2. Statistical Criteria to Determine the Optimal Number of Clusters.**

| Number of Clusters | $R^2$* | Semi-partial $R^2$† | Pseudo F statistic‡ |
|---|---|---|---|
| 2 | 0.166 | 0.124 | 66.194 |
| 3 | 0.290 | 0.062 | 67.812 |
| 4 | 0.352 | 0.046 | 59.991 |
| 5 | 0.398 | 0.041 | 54.614 |

*$R^2$ measures the heterogeneity of the cluster solution formed at a given step. A large value signifies that clusters at a given step are different from each other.

†Semi-partial $R^2$ measures the loss of homogeneity due to merging of 2 clusters to form a new cluster at a given step. A small value suggests that the cluster solution obtained at a given step is formed by merging of 2 very homogenous clusters.

‡Pseudo F statistic describes the ratio of between cluster variance to within cluster variance. Peak in the pseudo F statistic is indicative of large cluster separation.

**Table 3. Comparisons of Lamina Parameters in Three Clusters Obtained by a Hierarchical Cluster Analysis.**

| | Cluster 1 | Cluster 2 | Cluster 3 | | Post Hoc *P*† | | |
|---|---|---|---|---|---|---|---|
| | n = 89 | n = 130 | n = 116 | *P*-value* | 1 vs. 2 | 1 vs.3 | 2 vs. 3 |
| Lamina cribrosa depth, μm | 468.06 ± 109.84 | 546.40 ± 135.99 | 404.94 ± 95.45 | <0.0001 | <0.0001 | 0.0004 | <0.0001 |
| Lamina cribrosa thickness, μm | 166.05 ± 30.49 | 146.65 ± 30.34 | 201.69 ± 14.18 | <0.0001 | <0.0001 | <0.0001 | <0.0001 |

* *P*-value by analysis of variance among 3 clusters for variables.

† *P*-value by Turkey test for multiple testing between 2 clusters as post hoc test.

**Table 4. Comparisons of Parameters in Three Clusters Obtained by a Hierarchical Cluster Analysis.**

| Variables | Cluster 1 | Cluster 2 | Cluster 3 | | Post Hoc *P*† | | |
|---|---|---|---|---|---|---|---|
| | n = 89 | n = 130 | n = 116 | *P*-value* | 1 vs. 2 | 1 vs.3 | 2 vs. 3 |
| Age, y | 48.61 ± 11.88 | 65.07 ±13.44 | 49.51 ± 13.81 | <0.0001 | <0.0001 | 0.8782 | <0.0001 |
| Sex, male/female | 38/51 | 61/69 | 51/65 | 0.807 | >0.999 | >0.999 | >0.999 |
| Diagnosis (1/2/3) | 56/13/20 | 74/52/4 | 2/0/114 | <0.0001 | <0.0001 | <0.0001 | <0.0001 |
| Untreated IOP, mmHg | 16.68 ± 4.75 | 21.03 ± 9.50 | 12.53 ± 2.37 | <0.0001 | <0.0001 | <0.0001 | <0.0001 |
| IOP at scan day, mmHg | 13.84 ± 4.53 | 16.00 ± 7.65 | 12.51 ± 2.35 | <0.0001 | 0.0121 | 0.1971 | <0.0001 |
| Refractive errors, Diopters | -4.29 ± 2.52 | -0.19 ± 1.72 | 0.52 ± 1.40 | <0.0001 | <0.0001 | <0.0001 | 0.3654 |
| CCT, μm | 543.07 ± 42.21 | 560.45 ± 34.76 | 555.92 ± 36.83 | <0.0001 | 0.0025 | 0.0414 | 0.6136 |
| AXL, μm | 25.54 ± 1.04 | 23.60 ± 1.14 | 23.60 ± 0.93 | <0.0001 | <0.0001 | <0.0001 | 0.9999 |
| Average RNFL thickness, μm | 72.56 ± 18.76 | 67.09 ± 16.68 | 102.78 ± 8.80 | <0.0001 | 0.0241 | <0.0001 | <0.0001 |
| MD, dB | -7.70 ± 6.98 | -10.49 ± 9.22 | -0.34 ± 1.14 | <0.0001 | 0.0089 | <0.0001 | <0.0001 |

Diagnosis 1: Primary open angle glaucoma (POAG) with normal pressure, Diagnosis 2: POAG with high pressure, Diagnosis 3: Normal eyes.

IOP=Intraocular pressure, CCT=Central corneal thickness, AXL=Axial length, RNFL=Retinal nerve fiber layer, MD=Mean deviation.

* *P*-value by analysis of variance among 3 clusters for variables, in case of numeric Chi-square applied.

† *P*-value by Turkey test for multiple testing between 2 clusters as post hoc test.

**Table 5. Classification Tree Model Accuracy**

| | Cluster 1 | Cluster 2 | Cluster 3 |
|---|---|---|---|
| Prediction- Cluster 1 | 30 | 19 | 5 |
| Prediction-Cluster 2 | 29 | 95 | 0 |
| Prediction -Cluster 3 | 30 | 16 | 111 |

Classification tree accuracy = 0.704

**Table 6. Logistic Regression Analysis for Lamina Cribrosa Depth and Thickness Predicting Accuracy.**

| Variable | Coefficients | *P*-value | Odds-Ratio |
|---|---|---|---|
| Lamina cribrosa Depth | 0.0067 | 0.0004 | 1.0067 |
| Lamina cribrosa Thickness | -0.1011 | <0.0001 | 0.9038 |

Accuracy 298/335 = 89.0 %

**Figure 1. Measurement of Anterior Lamina Cribrosa Surface Depth and Lamina Cribrosa Thickness**

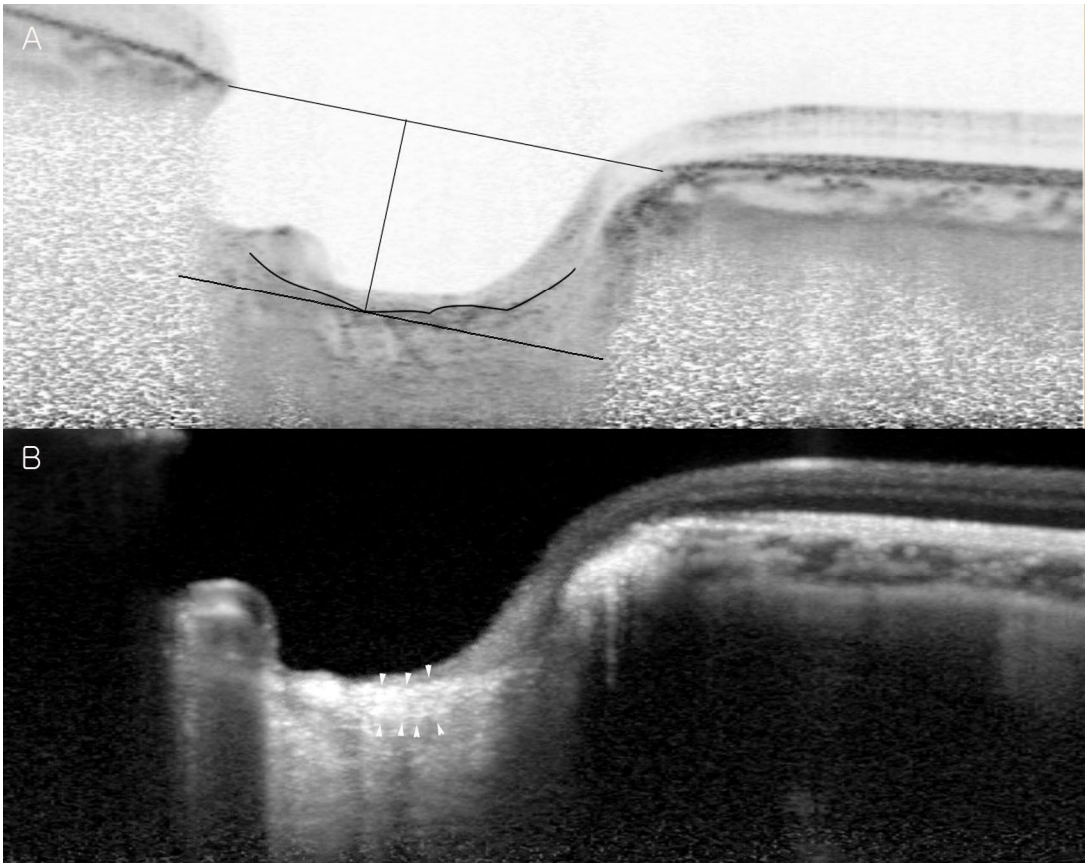


A. **Measurement of lamina cribrosa depth:** A smooth contour line was drawn following the anterior lamina cribrosa surface and the maximum depth was considered as the lamina cribrosa depth in each B-scan.

B. **Measurement of lamina cribrosa thickness:** Lamina cribrosa thickness was determined as the distance between the anterior and the posterior borders of the highly reflective region. When the anterior or posterior border of the lamina cribrosa was not definite on B scan image, the borders were determined by examining the en face images.

**Figure 2. Dendrogram that Shows Three Clusters Classified by Hierarchical Cluster Analysis**

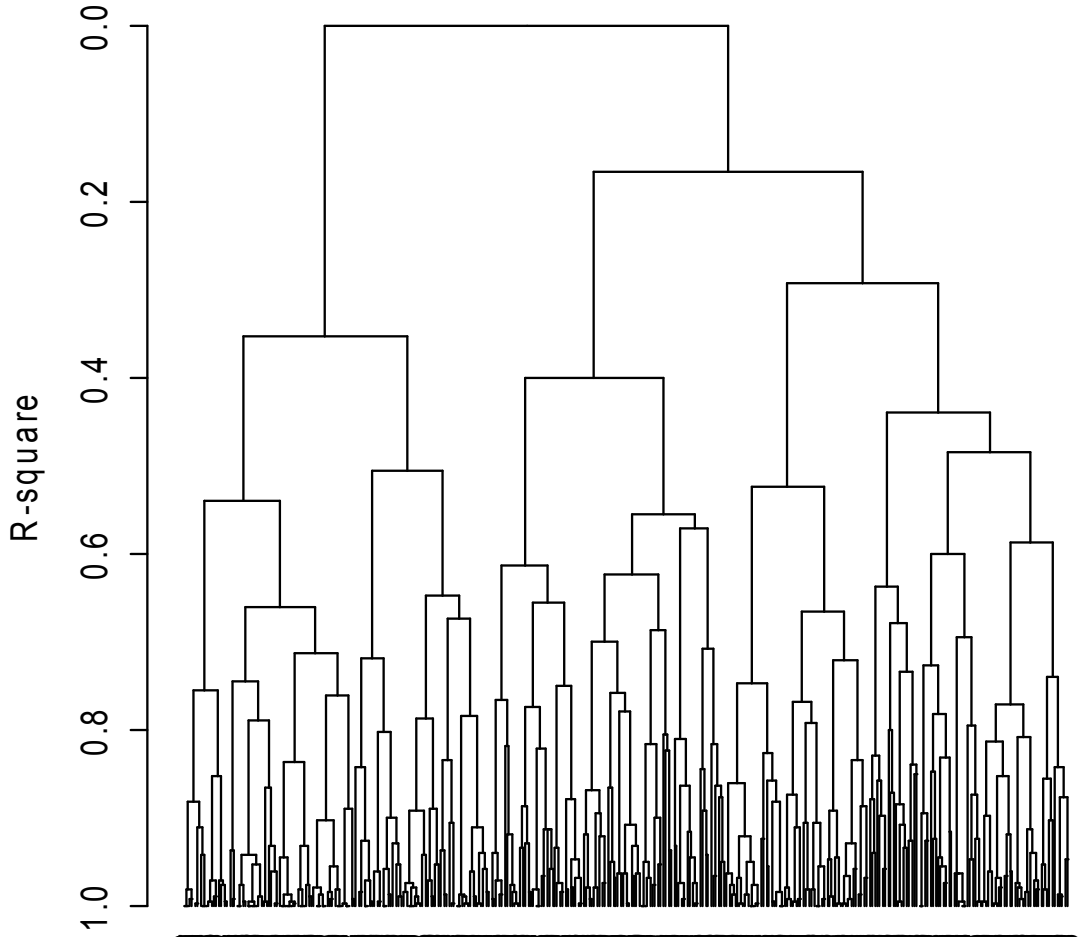


Dendrogram shows how clusters were made by the agglomerative technique, which began with each subject being a cluster by itself and merged together continuously based on similarity between clusters. When the number of cluster was 3, $R^2$ value which measured the heterogeneity of the cluster solution formed at a given step was 0.290.

**Figure 3. Classification Tree for Detecting Among Primary Open Angle Eyes.**

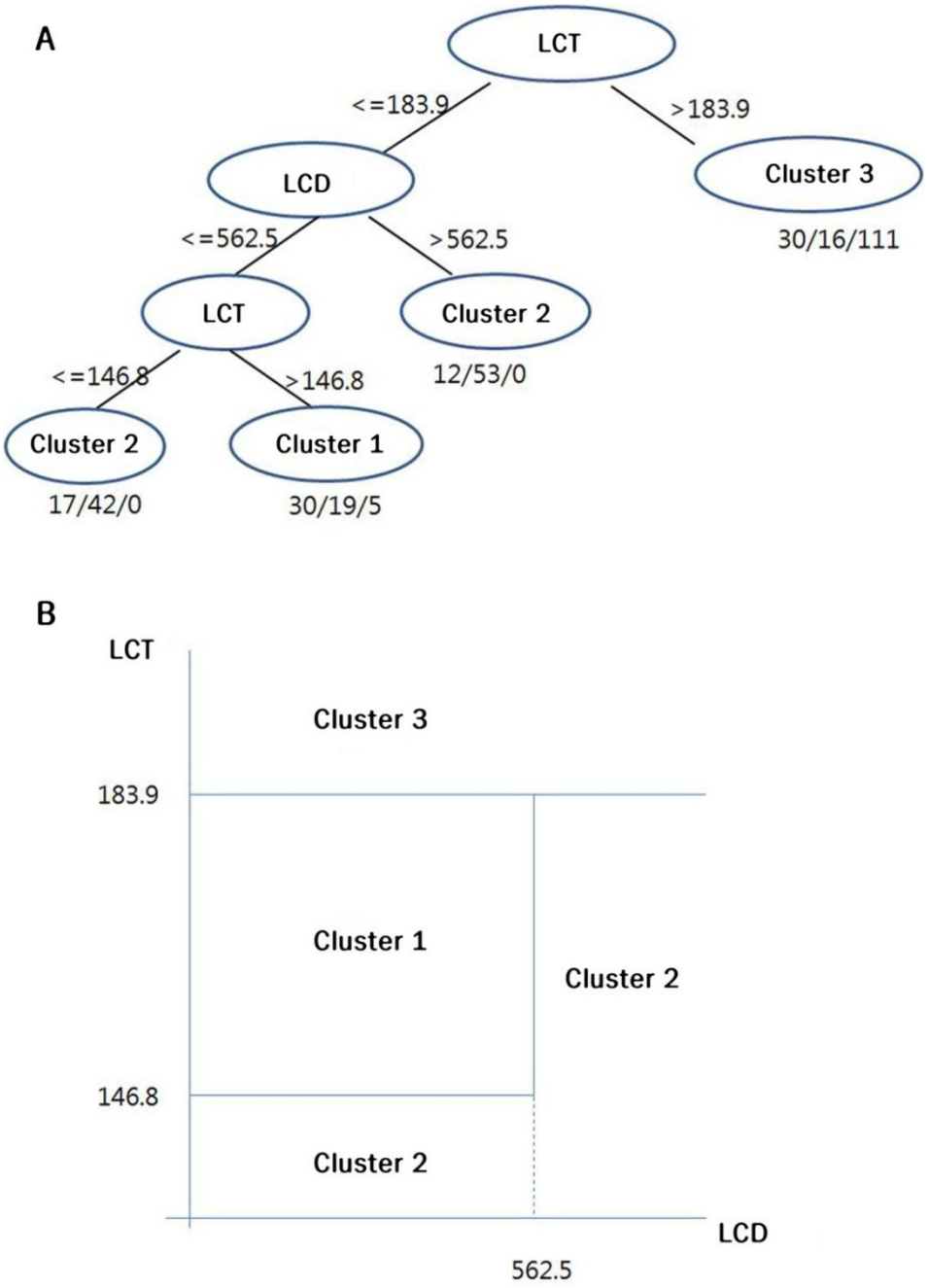


Classification tree was drawn. In brief, persons with LCT more than 183.9 μm can be categorized as cluster 3. Persons with LCT equal or less than 183.9 μm can be

categorized by LCD. Persons with LCD more than 562.5 μm can be classified as cluster 2. Of the remained persons, those with LCT more than 146.8 μm can be classified as cluster 1, those with LCT equal or less than 146.8 μm can be classified as cluster 2. This classification tree accuracy would be 0.704.

# 국 문 초 록

## 사상판 계측에 관한 연구 - 정상안과 녹내장안에서 사상판 깊이와 사상판 두께의 고찰

**목적**: 증강 깊이 이미징 기술을 이용한 스팩트럼 영역 빛간섭단층촬영으로 측정한 개방각 녹내장안과 정상안의 사상판깊이와 사상판두께를 분석하므로써 녹내장안의 병인과 관련이 있는 사상판의 특징에 따른 분류를 해보고자 한다.

**방법:** 본 연구에 정상안 138안과 개방각녹내장안 197안을 모집하여서 총 355안을 대상으로 하였다. 사상판을 측정하기 위하여 증강 깊이 이미징기술을 이용하여 스팩트럼 영역의 빛간섭단층촬영으로 시신경유두부의 연속되는 수평으로 스캔을 하였다. 사상판 깊이(기준점인 브룩스막 입구에서 사상판 앞면으로 수직으로 가장 깊은 선)과 사상판 두께를 시신경유두의 3군데에서 나누어서 각각 측정하였다. (위측 1/4 지점, 중앙, 하측 1/4 지점). 측정한 사상판깊이와 사상판두께를 이용하여 계층적 군집분석을 시행하였으며, 또한 로짓회귀분석을 시행하였다.

**결과**: 계층적 군집분석을 시행한 결과 통계적으로 유의한 3가지 군집으로 나눌 수 있었다. 군집 1은 군집 중에서 중간에 해당하는 사상판깊이 (468.06 μm)와 사상판두께 (166.05 μm)로 대변되는 특징을 보였다. 군집 중에서 군집 2는 가장 깊은 사상판깊이 (546.40 μm)와 가장 얇은 사상판두께 (146.65 μm)를 보였다. 군집 3은 가장 얕은 사상판깊이 (404.94 μm)와 가장 두꺼운 사상판두께 (201.69 μm)를 보였다. 녹내장발병과 관련된 인자로 알려진 나이, 치료 전 안압, 굴절력, 중심각막두께, 안축장 등의 인자를 군집간의 차이가 관찰되었다.

**결론**: 계층적 군집분석을 통해서 개방각 녹내장과 정상안에서 사상판깊이와 사상판두께로 3 가지 군집으로 나눌 수 있음을 알 수 있었다. 이러한 시도는 향후에 현재에 쓰이는 다소 자의적일 수도 있는 기존의 안압에 따른 녹내장 분류 이외에도 녹내장 병인에 중요한 사상판 특성에 의한 녹내장 분류법으로 향후 치료에 도움이 될 수 있으라고 기대한다.

**주 요 어: 사상판깊이, 사상판두께, 계층적 군집분석, 스팩트럼 영역빛간섭단층촬영, 녹내장**

**학 번: 2012-31123**